

Nexus sine qua non: Essentially Connected Networks for Traffic Forecasting

Tong Nie ¹, Guoyang Qin ¹, Yunpeng Wang ², Jian Sun ^{1*}

¹ Department of Traffic Engineering & Key Laboratory of Road and Traffic Engineering, Ministry of Education, Tongji University, Shanghai 201804, China,

² Beijing Key Laboratory for Cooperative Vehicle Infrastructure Systems and Safety Control, School of Transportation Science and Engineering, Beihang University, Beijing 100191, China,
 {nietong, 2015qgy, sunjian}@tongji.edu.cn; ypwang@buaa.edu.cn

Abstract

Spatial-temporal graph neural networks (STGNNs) have become the de facto models for learning spatiotemporal representations of traffic flow. However, modern STGNNs often contain superfluous or obscure components, along with complex techniques, posing significant challenges in terms of complexity and scalability. Such concerns prompt us to rethink the design of neural architectures and to identify the key challenges in traffic forecasting as spatial-temporal contextualization. Here, we present an essentially connected model based on an efficient message-passing backbone, powered by learnable node embedding, without any complex sequential techniques such as TCNs, RNNs, and Transformers. Intriguingly, empirical results demonstrate how a simple and elegant model with contextualization capability compares favorably w.r.t. the state-of-the-art with elaborate structures, while being much more interpretable and computationally efficient for traffic forecasting. We anticipate that our findings will open new horizons for further research to explore the possibility of creating simple but effective neural forecasting architectures.

1 Introduction

Modeling and forecasting spatiotemporal traffic flow not only facilitates decision making by practitioners, but also deepens our scientific understanding of the underlying dynamic systems. Spatiotemporal traffic forecasting (STTF) is one of the most popular applications of modern neural forecasting models, and numerous works have been devoted to developing advanced spatial-temporal graph neural networks (STGNNs) that can capture complex correlations in spatiotemporal traffic data (Yu, Yin, and Zhu 2018; Li et al. 2018; Wu et al. 2019b; Bai et al. 2020; Li et al. 2023).

Stacking multiple novel spatial-temporal layers tends to be a standardized practice in newly-emerged STGNNs. Despite improvements in accuracy in common benchmarks, the introduction of complex techniques and overly cumbersome architectures hinders the understanding of their behaviors and the discovery of components that really contribute to forecasting. It is dubious that the designs of some advanced STGNNs may conceptually complicate the forecasting process. Furthermore, increasing complexity often requires extensive training time and tedious parameter tuning, making

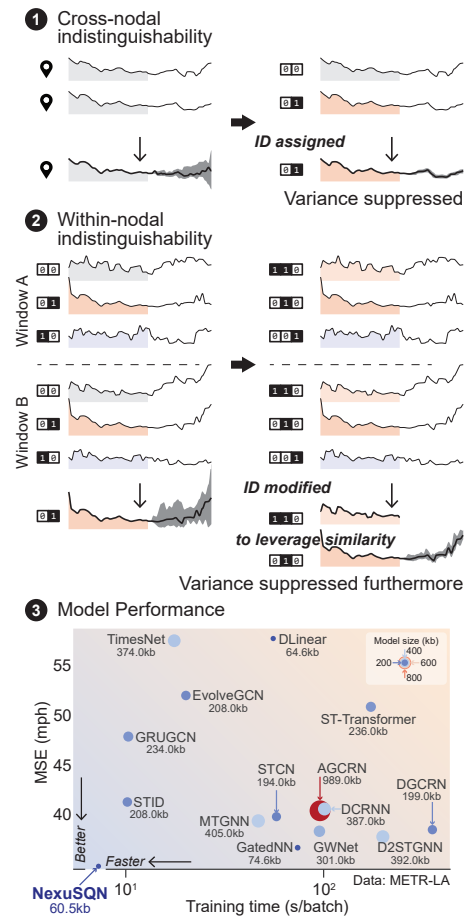


Figure 1: Illustration of the contextualization issue in spatiotemporal traffic data: ① if two future series that follow identical past series are different in two different sensors, then forecasting without knowing the location becomes indistinguishable; ② even at one location, if two series with identical past series are distinct at different times, the sensor identifier, since it remains constant, is no longer useful to distinguish the time-wise multivaluedness. ③ By exploiting the “where” and “when” loactors, our model can achieve favorable performance in both efficacy and efficiency.

*Corresponding author

many state-of-the-art models infeasible for large-scale sensor networks (Liu et al. 2023b; Jin et al. 2023).

The above phenomena prompt us to revisit the design of STGNNs and throw out an intriguing question: **Is there an essentially simple but effective model for STTF?** With this question, we first carefully inspect the STTF task. We find the forecasting can be particularly problematic when the future series is often nondeterministic with respect to the past series within a look-back window, which means that the maps to learn are one-to-many, and a deterministic one-to-one function, however expressive it is, cannot fully capture this multivalued mapping. This is especially difficult when there is no external information available to explain away the ambiguity. A key workaround is to reconstruct *contextualization* information from the data itself to separate “many” in a higher-dimensional space and turn the multivalued mapping into a univalued mapping. By contemplating the essence of the problem, we find that it basically involves injecting two essential elements corresponding to each of the multivalued mappings, which we call a “where locator” and a “when locator”, to contextualize the forecasting task in spatial and temporal dimensions, respectively (see Fig. 1).

Using the “where locator” and “when locator” lenses, we can focus on surveying models based on how they approach the two types of contextualization in a variety of studies. We then question the necessity and validity of using complex STGNNs for STTF and argue that many of them do not alleviate the contextualization problem but make it even more difficult to distinguish spatiotemporal samples. Given the complexity and inefficiency of current models, it may be tempting to go beyond such acknowledged paradigms and explore the performance of a minimalistic model that only includes essential connection components to directly express “where locator” and “when locator”.

To achieve this, we assign a unique vector as the “where locator” for each location. However, we do not assign additional vectors as “when locator” for each piece of time, as this would increase redundant parameters. Instead, we attempt to reuse the “where locator” as learnable embeddings to correlate past series of all sensors to contextualize the temporal location of the current series. Surprisingly, in our experiments, this reuse of the “where locator” as a “when locator” can perform comparatively with its complex counterparts while enjoying much faster training, less resource consumption, and fewer model parameters (see Fig. 1(3)). Our main contributions are threefold:

- We present a conceptually simple but effective model with essentially connected components for STTF;
- We identify and highlight the significance of node embedding in spatiotemporal contextualization;
- We conduct extensive experiments to evaluate the performance of the proposed model on 7 traffic forecasting benchmarks and reveal its superiority by comparing with 15 state-of-the-art neural forecasting models.

We hope that our results can encourage further work on this topic to go beyond the sphere of complex STGNNs and reconsider the significance of simpler models. As we aim to

grasp the most essential components for STTF, we refer to our model as *Nexus Sine Qua Non* (NexuSQN) networks.

2 Notations and Preliminary

Notations and problem statement We investigate the multivariate traffic forecasting problem in a spatiotemporal context. For ease of representation, we follow the terminology of previous work (Cini et al. 2022). In particular, N time series are collected from different static sensors, and each of them has a d_{in} dimensional traffic flow measurement, denoted by $\mathbf{x}_t^i \in \mathbb{R}^{d_{in}}$. The entire record at time t can be linked by sensor networks and forms a graph signal matrix $\mathbf{X}_t \in \mathbb{R}^{N \times d_{in}}$ with side information represented by the static adjacent matrix (possibly time varying) $\mathbf{A} \in \mathbb{R}^{N \times N}$. In addition, we indicate with the tensor $\mathcal{X}_{t:t+T} \in \mathbb{R}^{N \times T \times d_{in}}$ the sequence of graph signals within the time interval $[t, t + T]$. For STTF dataset, exogenous variables about time stamps are readily collected for the entire period, which is denoted as $\mathbf{U}_t \in \mathbb{R}^{N \times d_s}$. Similarly, node-specific features such as sensor ids are indicated as $\mathbf{V} \in \mathbb{R}^{N \times d_v}$. Note that this paper uses the terms nodes, sensors, and locations interchangeably. Input graph signals within a time window W can be denoted as $\mathcal{G}_{T-W:T} = \langle \mathcal{X}_{T-W:T}, \{\mathbf{U}_t, \mathbf{V}, \mathbf{A}_t, t = T - W, \dots, T\} \rangle$. The objective of STTF is to forecast the next H horizons of graph signals given a length of W historical records with a predictive function $F_\theta(\cdot)$: $\hat{\mathcal{G}}_{T+1:T+H} = F_\theta(\mathcal{G}_{T-W:T} | \theta)$.

Neural Message-passing of STGNNs GNNs can be considered as a general model of message-passing neural networks (MPNNs). MPNNs contain three forward computation phases: message passing (MP), feature aggregation, and node updating, parameterized by permutation-invariant functions (Gilmer et al. 2017). Under the spatiotemporal settings, MPNN at each time step can be formulated as follows:

$$\begin{aligned} \mathbf{m}_t^{i \leftarrow j, (l)} &= \text{MSG}_l(\mathbf{h}_t^{i, (l-1)}, \mathbf{h}_t^{j, (l-1)}, e_{i \leftarrow j}^t), \\ \mathbf{m}_t^{i, (l)} &= \text{AGG}(\mathbf{m}_t^{i \leftarrow j, (l)}; \forall j \in \mathcal{N}(i)), \\ \mathbf{h}_t^{i, (l)} &= \text{UP}_l(\mathbf{h}_t^{i, (l-1)}, \mathbf{m}_t^{i, (l)}), \end{aligned} \quad (1)$$

where $e_{i \leftarrow j}^t$ is the edge weight between node i and j at time t . An additional temporal MP process can be applied to model temporal correlations (Cini et al. 2023). Stacking several MPNNs or applying high-order ones can somewhat alleviate the spatial contextualization problem. However, these solutions are prone to the over-squashing problem (Dwivedi et al. 2022) and deficient in locating series in the time axis.

3 Essentially Connected Neural Predictors

The above discussion motivates us to develop a simple but effective model for STTF. We identify the key challenge of STTF as spatial and temporal contextualization and depend on the node embedding (NE) to learn distinguishable spatiotemporal representations. In particular, NexuSQN features an essentially connected neural architecture based on a message-passing backbone (see Fig. 2), and the rationale for NexuSQN is the versatile use of learnable node embedding and the simplicity of modular design. Notably, our model

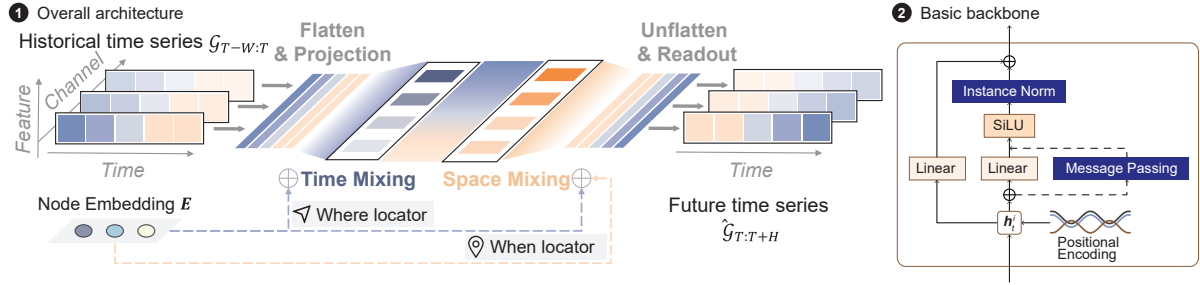


Figure 2: Architecture overview and basic block of NexusQN. Both TIMEMIXER and SPACEMIXER follow this backbone.

completely avoids complex temporal methods (e.g., RNNs, TCNs, and self-attention) and spatial techniques (e.g., diffusion convolutions and distance-based adjacent graphs) entirely. With a concise and comprehensible neural predictor, we seek to empirically answer the following key questions:

Q1 Are NE powerful for spatiotemporal contextualization?
Q2 With NE, how to keep the model structure minimalistic?
Q3 Are simplified model architectures effective for STTF?

With these questions, we provide detailed descriptions about each modular component in the following sections.

3.1 Overview of Architectural Components

Overview The overall architecture of NexusQN can be concisely formulated as follows:

$$\begin{aligned} \mathbf{H}_t^0 &= \text{PROJECTION}(\mathcal{X}_{t-W:t}), \\ \mathbf{H}_t^{(1)} &= \text{TIMEMIXER}(\mathbf{H}_t^{(0)}; \mathbf{E}_t), \\ \mathbf{H}_t^{(l+1)} &= \text{SPACEMIXER}(\mathbf{H}_t^{(l)}; \mathbf{A}), \quad l \in \{1, \dots, L\} \\ \mathcal{X}_{t:t+H} &= \text{READOUT}(\mathbf{H}_t^{(L+1)}), \end{aligned} \quad (2)$$

where TIMEMIXER and SPACEMIXER build on conceptually and technically simple MLP and MPNN blocks, which can be represented together by Fig. 2(2). \mathbf{E}_t is learnable NE, and \mathbf{A} is the relational graph. In the following paragraphs we will detail each component in turn.

Input flattening and PROJECTION STGNNs usually handle time and feature dimension separately, i.e., first project the input features at each time step to high-dimensional representations independently and correlate different time steps with sequential models like RNNs. Despite being reasonable and intuitive, this treatment increases the model complexity and the risk of overfitting significantly, especially when the hidden dimension is much larger than the channel (feature) dimension. As such, we proposed to flatten raw time series along time dimension and project the inputs into hidden space with a simple MLP layer:

$$\begin{aligned} \mathbf{X}_{t-W:t} &= \text{FOLD}([\mathcal{X}_{t-W:t} \| \mathbf{U}_t], \text{dim} = 0), \\ \mathbf{H}^0 &= \text{MLP}(\mathbf{X}_{t-W:t}), \end{aligned} \quad (3)$$

where $\text{FOLD}(\cdot) : \mathbb{R}^{N \times T \times d_{in}} \rightarrow \mathbb{R}^{N \times Td_{in}}$ is the flattening operation. By flattening and projecting along the time dimension, serial information is stored in the hidden state \mathbf{H}^0 . We further inject exogenous variables \mathbf{U}_t about series properties here to inform the projection layer with time-series information, e.g., periodicity and seasonality.

TIMEMIXER for exploiting historical information Time mixer models the temporal relations and patterns contained in historical series. We adopt 2-layer MLP with residual connection (He et al. 2016) to encode temporal representations:

$$\begin{aligned} \tilde{\mathbf{H}}^0 &= \text{SiLU}(\Theta_{\text{time}}^0 \mathbf{H}^0), \\ \mathbf{H}^1 &= \text{IN}(\Theta_{\text{time}}^1 \tilde{\mathbf{H}}^0) + \Theta_{\text{time}}^0 \mathbf{H}^0, \end{aligned} \quad (4)$$

where $\Theta_{\text{time}}^0, \Theta_{\text{time}}^1$ are linear weights, $\text{IN}(\cdot)$ is the instance normalization (Ulyanov, Vedaldi, and Lempitsky 2016), which is adopted to mitigate distribution shift (Kim et al. 2021; Nie et al. 2022) and reinforce the representations of high-frequency temporal components (Deng et al. 2021).

SPACEMIXER for modeling relational information The proposed graph mixer can be viewed as a structured feature (channel) mixing layer, which is a specialization of the vanilla MLP mixer (Chen et al. 2023). As shown in Fig. 2, what differentiates SPACEMIXER from TIMEMIXER is the MP step that aggregates neighborhood features on graphs.

Considering the dependence of channels (sensors), the MLP mixer can be formulated as:

$$\mathbf{H}^{(l)} = \sigma(\Theta_{\text{channel}}^{(l)} \mathbf{H}^{(l-1)} \Theta_{\text{time}}^{(l)}), \quad (5)$$

where Θ_{feature} is the channel mixing weight and can also be interpreted as an unconstrained graph learning module that contains N^2 parameters. To specialize this model, we adopt a structured MPNN as the featured block of graph mixer:

$$\text{MPNN}^{(l)}(\mathbf{H}^{(l-1)}; \mathbf{A} | \Theta) = \text{SiLU}(\mathbf{A} \mathbf{H}^{(l-1)} \Theta_{\text{time}}^{(l)}), \quad (6)$$

where \mathbf{A} is the relational graphs, which can be either a priori ones or adaptively learned. It can be seen that our graph mixer exploits the characteristics of adjacent matrices and explicitly models the pairwise interactions among nodes. By seizing relational information, our model achieves a modular extension from univariate models to multivariate.

Dense READOUT For multi-step STTF, we adopt a MLP and reshaping layer to directly output the predictions:

$$\begin{aligned} \hat{\mathbf{X}}_t &= \text{MLP}(\mathbf{H}_t^{(L)}), \\ \hat{\mathcal{X}}_{t:t+H} &= \text{UNFOLD}(\hat{\mathbf{X}}_t), \end{aligned} \quad (7)$$

where $\text{UNFOLD}(\cdot)$ is the inverse linear operator of $\text{FOLD}(\cdot)$. Again, we do not elaborate on a complex sequential decoder, and the multistep predictions are regressed directly.

3.2 Node Embedding for When-Where Contextualization

One cornerstone of the proposed framework is the versatility of NE. To tackle the spatial-temporal contextualization issue, the roles of NE in our model are twofold, including: *where locator* and *when locator*, which correspond to positional and structural representation in the theory of GNNs' representation learning (Srinivasan and Ribeiro 2019).

Spatial-temporal node embedding For the space dimension, we consider setting a unique identifier for each sensor. An optional structural embedding is the random-walk diffusion matrix (Dwivedi et al. 2020). For simplicity, we use the learnable NE as a simple index positional encoding without any structural priors. As for implementation, we assign a learnable vector of size d_{emb} with random initialization for each series, denoted as $\mathbf{E} \in \mathbb{R}^{N \times d_{emb}}$, then \mathbf{E} is included in the forward computation as endogenous variables and its gradient is updated end-to-end by backpropagation.

This NE reflects the static features of each sensor, e.g., dominating traffic patterns (Nie et al. 2023a), and is agnostic to temporal information. Inspired by (Marisca, Cini, and Alippi 2022), we propose to inform the model with stationary serial property of traffic flows, e.g., periodicity and seasonality. The sinusoidal positional encoding (Vaswani et al. 2017) $\mathbf{U}_t \in \mathbb{R}^{T \times d_s}$ is adopted to inject the time-of-day information to all series. Given \mathbf{U}_t , we first fold the time dimension and project it into the hidden space:

$$\begin{aligned} \tilde{\mathbf{u}} &= \mathbf{W}_U \text{FOLD}(\mathbf{U}_t), \\ \tilde{\mathbf{U}} &= \text{BROADCAST}(\tilde{\mathbf{u}}, N), \\ \mathbf{E}_t &= \text{RESMLP}(\text{RESMLP}(\mathbf{E} + \tilde{\mathbf{U}})), \end{aligned} \quad (8)$$

where $\mathbf{W}_U \in \mathbb{R}^{d_{emb} \times T d_s}$ is learnable weights, and $\text{BROADCAST}(\cdot)$ duplicates the inputs with given times along a new dimension. \mathbf{E}_t is the final spatiotemporal node embedding (STNE). Since input data from different time-of-day intervals has different sinusoidal stamps, STNE can reflect periodicity of series. The following paragraphs explain how this STNE contributes to the traffic forecasting process.

“Where locator” It can be seen that Eqs. 4 and 6 are global models shared by all sensors. Given two sensors with similar historical inputs, such global models fail to contextualize each series in the spatial dimension, even though they have different dynamics in the future. To circumvent such a one-to-many problem, we parameterize each node with a discriminative identifier using the STNE. Especially, we add the learnable \mathbf{E}_t to each series in the first MLP of TIMEMIXER as spatial contextualization directly:

$$\tilde{\mathbf{h}}_i^0 = \text{MLP}(\mathbf{h}_i^0 + \mathbf{e}_i). \quad (9)$$

Notably, the introduction of learnable embedding in each node is shown to be equivalent to the specialization of the univariate model (Cini et al. 2023), which benefits the use of node-specific local dynamics (Sen, Yu, and Dhillon 2019).

On the other hand, since GNNs focus on local graph structures, they are inadequate to distinguish between two nodes with close neighborhood structure, which is understood as

a spatial indistinguishability problem (Dwivedi et al. 2022). Therefore, to allow the aggregation function to be aware of the difference of each node, so that the node features can still be discriminated after the message aggregation, we include \mathbf{E}_t in the MP process in Eq. 1:

$$\mathbf{m}_t^{i \leftarrow j} = \text{MSG} \left(\begin{bmatrix} \mathbf{h}_t^i \\ \mathbf{e}^i \end{bmatrix}, \begin{bmatrix} \mathbf{h}_t^j \\ \mathbf{e}^j \end{bmatrix}, a_{i \leftarrow j}^t \right). \quad (10)$$

We claim that adding learnable features to the message function is equivalent to incorporating high-frequency components into low-frequency representations to highlight the impact of local events in spatiotemporal data. Actually, the random node initialization itself enhances the GNNs (Sato, Yamada, and Kashima 2021). As can be seen, the “where locator” only implies the exclusivity of the identifier, we set it to be learnable for the sake of reuse for the “when locator”.

“When locator” STNE represents the dominant traffic flow patterns and can be understood as a global and static identifier. If a sensor's readings are different at two different times but share a close historical series, the “where locator” alone is less effective at contextualizing its temporal information. In this case, an additional “when locator” is needed.

Following the discussions in (Chen et al. 2023), we can first divide forecasting models into two categories according to their encoding mechanisms: (1) time-dependent and (2) data-dependent. Concretely, a linear predictive model with weight \mathbf{W} and bias \mathbf{b} can be expressed as:

$$\begin{aligned} \mathbf{x}_{t+1:t+H} &= \mathbf{W} \mathbf{x}_{t-W:t} + \mathbf{b}, \\ \text{or: } x_{t+h} &= \sum_{k=0}^W w_{k,h} x_{t-k} + b_{k,h}, \quad h \in \{1, \dots, H\}, \end{aligned} \quad (11)$$

which forms a vanilla autoregressive (AR) model at each forecast horizon, where the AR parameters depend only on the relative order and are agnostic to the location in the historical sequence. The TIMEMIXER works in this way.

One natural “when locator” for time-dependent model is to assign a unique identifier to each piece of time. However, there exists three drawbacks: (1) since the prediction is basically done sequence-to-sequence, having different identifiers within a time window is redundant; (2) the time-dependent model in Eq. 11 relies on relative timestamps and the use of absolute ones is difficult for it; (3) timestamp-based encoding would attribute the ambiguity to time-varying factors, e.g., rush hour, but this may be caused by local high-frequency spatial dynamics such as the spread of traffic congestion or irregular driving behavior.

Conversely, the behaviors of data-dependent models are pattern-aware and condition on local temporal variations:

$$x_{t+h} = \sum_{k=0}^W \mathcal{F}_k(\mathbf{x}_{t-W:t}) x_{t-k} + b_{k,h}, \quad h \in \{1, \dots, H\}, \quad (12)$$

where $\mathcal{F}_k(\cdot)$ is a data-driven function, e.g., self-attention. We argue that this forms a fully time-varying AR model (Bringmann et al. 2017) in which the AR process is parameterized by time-varying coefficients. This overparameterization tends to overfit the data rather than capture the temporal relationships such as the location on the time axis.

With this in mind, we propose to reuse the “where locator” as a query for all available reference information from other series to contextualize the temporal patterns. In essence, we only need to specify the relation graphs in Eq. 6:

$$\mathbf{A}_t = \text{SOFTMAX}(\mathbf{E}_t \cdot \mathbf{E}_t^\top). \quad (13)$$

Since \mathbf{E}_t is aware of the time-of-day feature, this query function is time-varying within a period. Our approach lies between the time-dependent and data-dependent routines and can forecast with both relative time stamp and local spatial patterns. In this way, the positional node embeddings and structural graph representations are equivalently unified (Srinivasan and Ribeiro 2019) in spatiotemporal graphs.

3.3 Remarks on Parameter-Efficient Neural Message-Passing Designs

Another ingenuity of NexusQN is its parameter-efficient MP backbone. We present several task-agnostic techniques to lighten the overall neural architecture. Note that since NexusQN propagates features only after the temporal encoder, rather than at every time step, it is more efficient than alternately stacked spatial-temporal blocks.

Residual connection We keep a shortcut for the linear part in each block. When all residual connections are activated (e.g., when graph relation is unnecessary), our model can degenerate into a class of linear models with channel-independence, e.g., (Zeng et al. 2022; Das et al. 2023), which show great potential for long-term series forecasting.

Parameter sharing Different from recent design trends that assign different node parameters or graphs for different layers (Zhang et al. 2020; Oreshkin et al. 2021), we set the NE globally shared for all modules. The idea is to facilitate end-to-end training of random node features and reduction of model size. In addition, recent works empirically show that MLPs and MPNNs can share similar feature spaces (Yang et al. 2022; Han et al. 2022). Without MP, SPACEMIXER can collapse into TIMEMIXER. Considering this, we instantiate the successive MP layers with a common linear transform for time mixing.

Shallow-layer structure Instead of multilayer deep GNN structures, we adopt shallow-layer structures with larger receptive field. In particular, we consider using one or two layers of MPNN with fully connected graphs to capture long-range spatial dependence, without multiple stacked sparse graph aggregators or hierarchical operations, e.g., diffusion graph convolutions (Li et al. 2018). Recent studies reveal that the expressive power of GNNs are determined by both of the depth and width (Loukas 2019), and wider GNNs can be more expressive than deeper ones (Wu et al. 2019a). A single MP can gather adequate information from a large number of nodes when the underlying graph is dense (Baranwal, Fountoulakis, and Jagannath 2023).

4 Related Works

Spatiotemporal traffic forecasting has sparked great interest in both academia and industry. As a standard paradigm,

STGNNs take all series as input and use GNNs to correlate them. The properties of traffic flow series are preserved by an elaborate sequential model. Remarkable results have been achieved in a variety of studies using STGNNs (Yu, Yin, and Zhu 2018; Li et al. 2018; Wu et al. 2019b; Bai et al. 2020; Guo et al. 2019; Zheng et al. 2020). However, modern STGNNs tend to be complex and nontrivial to implement.

Research on simplified deep models for STTF has been relatively limited. Cini et al. (2022) propose a scalable STGNN based on preprocessing that encodes spatiotemporal features prior to training. Liu et al. (2023a) replace the GNNs with feature aggregation and use a graph sampling strategy. While, both of them rely on complex temporal encoders and pre-computed graph features. Similarly to our work, Satorras, Rangapuram, and Januschowski (2022) developed a fully connected gated GNN model (GatedGN) using a graph inference structure. However, all pairwise attention is computationally very expensive. Along another path of research, several methods have emerged to challenge the existing complex models for LTSF, e.g., LightTS (Zhang et al. 2022), LTSF-Linear (Zeng et al. 2022), TS-Mixer (Chen et al. 2023) and TiDE (Das et al. 2023). While most adopt a channel-independence assumption and do not include explicit relational modeling.

Regarding positional encoding in STGNNs, Shao et al. (2022a) applies learnable embedding to all nodes, time of day, and day of week points, enabling MLPs to achieve competitive performance on multiple datasets. However, over-parameterized identifiers would be redundant and prone to overfit. Additionally, this kind of temporal identifier only reflect time-varying components and is less effective in capturing local nonstationary spatial dynamics. Cini et al. (2023) further interpreted the role of node embedding as local effects and incorporated it into a global-local architecture.

In summary, none of the existing works has directly and thoroughly investigated the essential model components for spatiotemporal traffic forecasting, nor provided exhaustive discussions on the contextualization issue in STGNNs.

5 Empirical Evaluation

Extensive experiments are carried out to evaluate the performance of the NexusQN model on 7 well-known traffic forecasting benchmarks and compare it with 15 neural forecasting baselines. Details about experimental settings are provided in the Appendix. **PyTorch implementations and reproducible results are publicly available [code]¹.**

5.1 Experiment Setup

Datasets Six high resolution traffic flow datasets are used to compare short-term forecast performance, including two traffic speed data: METR-LA and PEMS-BAY datasets (Li et al. 2018), and four traffic volume data (Guo et al. 2021): PEMS03, PEMS04, PEMS07, and PEMS08. All these traffic measurements are obtained from loop sensors installed on highway networks and aggregated at 5 min. In particular, the six datasets provide adjacent matrices constructed by the pairwise geographic distance between sensors. The same

¹Code will be open-sourced upon publication.

DATASET	METR-LA						PEMS-BAY						PEMS03														
	15 min			30 min			60 min			15 min			30 min			60 min			15 min			30 min			Average		
METRIC	MAE	MAE	MAE	MAE	MSE	MAPE (%)	MAE	MAE	MAE	MAE	MSE	MAPE (%)	MAE	MAE	MSE	MAPE (%)	MAE	MAE	MAE	MAE	MAE	MAE	MAE	MAPE (%)	Average	Average	
AGCRN	2.85	3.19	3.56	3.14	40.94	8.69	1.38	1.69	1.94	1.63	13.59	3.71	14.65	15.72	16.82	15.58	15.08										
DCRNN	2.81	3.23	3.75	3.20	41.12	8.90	1.37	1.72	2.09	1.67	14.52	3.78	14.59	15.76	18.18	15.90	15.74										
GWNet	2.74	3.14	3.58	3.09	38.86	8.52	1.31	1.65	1.96	1.59	13.31	3.57	13.67	14.60	16.23	14.66	14.88										
GatedGN	2.72	3.05	3.43	3.01	37.19	8.20	1.34	1.65	1.92	1.58	13.17	3.55	13.72	15.49	19.08	17.08	14.44										
GRUGCN	2.93	3.47	4.24	3.46	48.47	9.85	1.39	1.81	2.30	1.77	16.70	4.03	14.63	16.44	19.87	16.62	15.96										
EvolveGCN	3.27	3.82	4.59	3.81	52.64	10.56	1.53	2.00	2.53	1.95	18.98	4.43	17.07	19.03	22.22	19.11	18.61										
ST-Transformer	2.97	3.53	4.34	3.52	51.49	10.06	1.39	1.81	2.29	1.77	17.01	4.09	14.03	15.72	18.74	15.85	15.37										
STCN	2.84	3.25	3.80	3.23	40.34	9.02	1.37	1.71	2.08	1.66	14.11	3.75	14.27	15.49	18.02	15.61	16.07										
STID	2.82	3.18	3.56	3.13	41.83	9.07	1.32	1.64	1.93	1.58	13.05	3.58	13.88	15.26	17.41	15.27	16.39										
MTGNN	2.79	3.12	3.46	3.07	39.91	8.57	1.34	1.65	1.91	1.58	13.52	3.51	13.74	14.76	16.13	14.70	14.90										
D2STGNN	2.74	3.08	3.47	3.05	38.30	8.44	1.30	1.69	1.89	1.55	12.94	3.50	13.36	14.45	15.96	14.45	14.55										
DGCRN	2.73	3.10	3.54	3.07	39.02	8.39	1.33	1.65	1.95	1.59	13.12	3.61	14.34	15.54	17.53	15.52	15.20										
SCINet	3.06	3.47	4.09	3.47	44.61	9.93	1.52	1.85	2.24	1.82	14.92	4.14	14.39	15.25	17.37	15.43	15.37										
NexuSQN	2.65	2.99	3.37	2.95	35.10	8.05	1.30	1.60	1.86	1.53	12.22	3.42	13.26	14.27	15.82	14.25	14.12										

- Best results are bold marked. Note that - indicates the model runs out of memory with the minimum batch size.

Table 1: Results on METR-LA, PEMS-BAY, PEMSO3, PEMSO4, PEMSO7, and PEMSO8 datasets. MAE for 15, 30, 60 minutes forecasting horizons, as well as MAE, MSE, and MAPE averaged over a one hour (12 steps) are reported.

graphs from previous work (Wu et al. 2019b; Marisca, Cini, and Alippi 2022) are prepared for baselines that require pre-defined graphs. Then we evaluate the scalability and the ability to forecast long-term series on the `TrafficL` benchmark (Lai et al. 2018), which provides records of hourly road occupancy rates measured by 862 sensors for 48 months on San Francisco Bay Area freeways. Detailed descriptions of these benchmarks are given in Appendix.

Baselines We consider a variety of deep learning baselines in the literature to benchmark our model: AGCRN (Bai et al. 2020); DCRNN (Li et al. 2018); GWNet (Wu et al. 2019b); GatedGN (Satorras, Rangapuram, and Januschowski 2022); GRUGCN (Gao and Ribeiro 2022); EvolveGCN (Pareja et al. 2020); ST-Transformer (Xu et al. 2020); STCN (Yu, Yin, and Zhu 2018); STID (Shao et al. 2022a); MTGNN (Wu et al. 2020); D2STGNN (Shao et al. 2022b); SCINet (Liu et al. 2022); DGCRN (Li et al. 2023); DLinear (Zeng et al. 2022); TimesNet (Wu et al. 2022). To give a fair comparison, we use the official implementations in their original papers and use the recommended hyper-parameters on each dataset as far as possible. All baselines are evaluated under the same training, validation, and testing environments.

Experimental settings We follow the same experiment setups as used in previous works whatever possible to provide unbiased evaluations. For six short-term datasets, we use 12-step historical series (1 hour) to forecast future 12-step observations. For large-scale `TrafficL` data, we adopt the settings in (Wu et al. 2022) that 96 steps are used as input and predictions at next {96, 192, 288, 384} steps are

used for evaluation. Quantitative metrics including mean absolute error (MAE), mean squared error (MSE), and mean absolute percentage error (MAPE) are calculated.

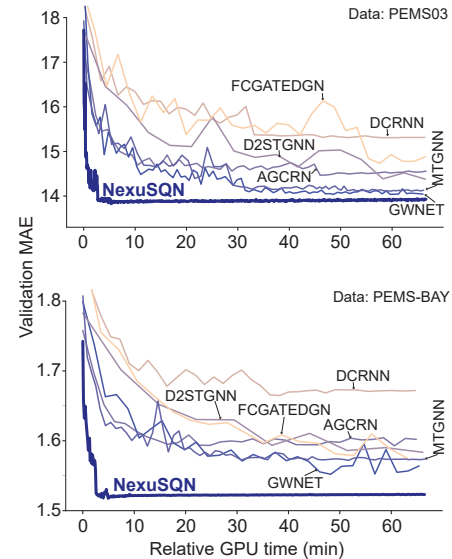


Figure 3: Validation MAE curves of different models.

5.2 Results

Short-term traffic benchmarks Model comparison results on six short-term speed and volume benchmarks are

given in the Tab. 1. Intriguingly, NexusQN has achieved performances comparable to or better than its other complicated counterparts. In particular, forecasting METR-LA data is supposed to be more challenging due to complex temporal patterns, while our model consistently outperforms baselines by a large margin, even without popular sequential techniques (**Q3**). For PEMS-BAY data, NexusQN is still among the best-performing predictors. Compared to STID, our model features the extraction of distinguishable low-frequency node representations with more effective “when locators”, thus showing better accuracy in all scenarios. Additionally, attention-based methods such as GatedGN, MT-GNN, and D2STGNN also show competitive results. However, high memory consumption and computational complexity hinder them from large-scale applications.

Similar observations can be made in the traffic volume datasets. Although NexusQN does not depend on a predefined adjacent matrix, it still achieves SOTA performance. Unlike the loop speed, distance-based correlation metrics may fail to describe the behavior of traffic volumes (Nie et al. 2023b). Our observation further confirms this claim. It is worth commenting that PeMS07 contains more than eight hundred sensors, so that the attention mechanism on the spatial dimension will lead to a prohibitive memory cost. Finally, with spatiotemporal contextualization, NexusQN can take advantage of relational information to improve forecasting with a simple structure (**Q1**).

	METR-LA				PEMS-BAY			
	Speed (Batch/s)	Memory (GB)	Batch size	Model size (k)	Speed (Batch/s)	Memory (GB)	Batch size	Model size (k)
AGCRN	10.43	4.1	64	989	6.78	6.0	64	991
DCRNN	9.90	3.8	64	387	6.72	5.5	64	387
GWNet	10.50	3.4	64	301	7.11	5.0	64	303
FC-Gated-GN	13.53	6.0	32	74.6	11.27	7.1	16	82.2
GRUGCN	97.09	2.5	64	234	56.51	2.9	64	234
EvolveGCN	49.66	1.8	64	208	38.36	2.2	64	208
ST-Transformer	5.77	8.2	64	236	6.63	7.6	32	236
STCN	17.31	2.9	64	194	12.05	3.8	64	194
STID	98.18	1.6	64	208	77.81	1.7	64	230
MTGNN	21.39	2.9	64	405	13.54	4.9	64	573
D2STGNN	5.02	6.9	32	392	5.38	7.0	16	394
DGCNN	2.82	8.0	64	199	2.74	6.9	32	208
SCINet	76.72	2.6	64	121	78.12	2.7	64	316
NexusQN	137.35	1.2	64	60.5	90.26	1.3	64	75.6

Table 2: Model computational performances.

Computational performance Apart from results on forecasting precision, we also examine the computational performance. Fig. 3 displays the validation MAE curves of several competing STGNNs on two datasets. Records of training speed, model size and memory usage on METR-LA are exemplified in Tab. 2. Notably, NexusQN enjoys a much faster training speed (converge in ten minutes of GPU time), smoother convergence curve, lower error bound, and less training expense, indicating high efficiency and scalability. This superiority is achieved through a technically simple structure, node embedding reuse, and parameter-efficient backbones (**Q2**). Advanced STGNNs like DGCNN, D2STGNN apply a series of alternating graph convolution and temporal models, resulting in a high computational burden and unstable optimization. Extra operations such as self-attention or graph attention further complicate the process.

Table 3: Long-term horizon forecasting results.

TrafficCL	Models	NexusQN	DLinear	TimesNet	SCINet
	Metric	MAE ($\times 10^{-2}$)	MAE	MAE	MAE
96	96	1.206	1.299	1.312	1.207
	192	1.273	1.407	1.411	1.398
	288	1.280	1.739	1.434	1.410
	384	1.345	1.921	1.521	1.471
Ave.	NMAE	1.752	2.144	1.883	1.855
	MRE (%)	21.03	25.73	22.60	22.27
	MAPE (%)	41.03	46.22	44.87	50.33

- Note that we do not use normalization on the raw data and report the original metrics.

Long-term forecasting performances We also examine the ability to predict long-term series. Tab. 3 reports the results of different prediction horizons with a 96-step sequence as input. Compared to three strong baselines in the LTSF literature, NexusQN shows great potential to handle the challenging LTSF task. This may be because our model can encode series with both relative time stamp and local patterns.

Table 4: Ablation studies on METR-LA and PEMS03 data.

Variations	METR-LA			PEMS03		
	w/o E	w \mathbf{A}_{pre}	w \mathbf{S}_{emb}	w/o E	w \mathbf{A}_{pre}	w \mathbf{S}_{emb}
Metric	MAE	MAE	MAE	MAE	MAE	MAE
15 min	2.88	2.64	2.84	14.85	13.48	14.64
30 min	3.32	2.98	3.23	16.62	14.54	15.91
60 min	3.76	3.38	3.65	18.68	15.95	17.45
Ave	MAE	3.25	2.95	3.18	16.46	14.45
	MSE	39.97	35.89	39.40	766.64	610.47
						676.63

Ablation study We conduct ablation studies to test the rationality of model designs. Tab. 4 reports the forecasting performance of different model variations: w/o E indicates the node embedding is removed and NexusQN degrees into a MLP-mixer; w \mathbf{A}_{pre} incorporates the predefined graphs with additional diffusion graph convolution (Li et al. 2018); w \mathbf{S}_{emb} means that we replace the STNE with timestamp-based embedding. The results clearly confirm the essence of the model designs and corroborate our hypothesis (**Q1, Q2**).

6 Conclusion and Outlook

This work goes beyond the realm of STGNNs and demonstrates an essentially connected network NexusQN for traffic forecasting. We identify the core challenge of STTF as spatial-temporal contextualization issue and design “where” and “when” locators to tackle it. NexusQN features a simple structure and a parameter-efficient backbone. Extensive and rigorous evaluations on several benchmarks indicate that NexusQN not only outperforms a diverse array of baselines but also enjoys high computational efficiency. We believe that NexusQN will form the basis for further research on understanding and designing simpler neural forecasting models and will help practitioners develop more efficient tools in industrial applications. Future work includes further exploration of performance on larger-scale datasets and a wider variety of data, as well as the interpretability.

Acknowledgments

This research was sponsored by the National Natural Science Foundation of China (52125208), and the Science and Technology Commission of Shanghai Municipality (No. 22dz1203200).

References

Bai, L.; Yao, L.; Li, C.; Wang, X.; and Wang, C. 2020. Adaptive graph convolutional recurrent network for traffic forecasting. *Advances in neural information processing systems*, 33: 17804–17815.

Baranwal, A.; Fountoulakis, K.; and Jagannath, A. 2023. Effects of graph convolutions in multi-layer networks. In *The Eleventh International Conference on Learning Representations*.

Bringmann, L. F.; Hamaker, E. L.; Vigo, D. E.; Aubert, A.; Borsboom, D.; and Tuerlinckx, F. 2017. Changing dynamics: Time-varying autoregressive models using generalized additive modeling. *Psychological methods*, 22(3): 409.

Chen, S.-A.; Li, C.-L.; Yoder, N.; Arik, S. O.; and Pfister, T. 2023. Tsmixer: An all-mlp architecture for time series forecasting. *arXiv preprint arXiv:2303.06053*.

Cini, A.; Marisca, I.; Bianchi, F. M.; and Alippi, C. 2022. Scalable Spatiotemporal Graph Neural Networks. *arXiv preprint arXiv:2209.06520*.

Cini, A.; Marisca, I.; Zambon, D.; and Alippi, C. 2023. Tamming Local Effects in Graph-based Spatiotemporal Forecasting. *arXiv preprint arXiv:2302.04071*.

Das, A.; Kong, W.; Leach, A.; Sen, R.; and Yu, R. 2023. Long-term Forecasting with TiDE: Time-series Dense Encoder. *arXiv preprint arXiv:2304.08424*.

Deng, J.; Chen, X.; Jiang, R.; Song, X.; and Tsang, I. W. 2021. St-norm: Spatial and temporal normalization for multi-variate time series forecasting. In *Proceedings of the 27th ACM SIGKDD conference on knowledge discovery & data mining*, 269–278.

Dwivedi, V. P.; Joshi, C. K.; Luu, A. T.; Laurent, T.; Bengio, Y.; and Bresson, X. 2020. Benchmarking graph neural networks. *arXiv preprint arXiv:2003.00982*.

Dwivedi, V. P.; Luu, A. T.; Laurent, T.; Bengio, Y.; and Bresson, X. 2022. Graph Neural Networks with Learnable Structural and Positional Representations. In *International Conference on Learning Representations*.

Gao, J.; and Ribeiro, B. 2022. On the Equivalence Between Temporal and Static Equivariant Graph Representations. In *International Conference on Machine Learning*, 7052–7076. PMLR.

Gilmer, J.; Schoenholz, S. S.; Riley, P. F.; Vinyals, O.; and Dahl, G. E. 2017. Neural message passing for quantum chemistry. In *International Conference on Machine Learning*, 1263–1272. PMLR.

Guo, S.; Lin, Y.; Feng, N.; Song, C.; and Wan, H. 2019. Attention based spatial-temporal graph convolutional networks for traffic flow forecasting. In *Proceedings of the AAAI Conference on Artificial Intelligence*, volume 33, 922–929.

Guo, S.; Lin, Y.; Wan, H.; Li, X.; and Cong, G. 2021. Learning dynamics and heterogeneity of spatial-temporal graph data for traffic forecasting. *IEEE Transactions on Knowledge and Data Engineering*, 34(11): 5415–5428.

Han, X.; Zhao, T.; Liu, Y.; Hu, X.; and Shah, N. 2022. MLPInit: Embarrassingly Simple GNN Training Acceleration with MLP Initialization. *arXiv preprint arXiv:2210.00102*.

He, K.; Zhang, X.; Ren, S.; and Sun, J. 2016. Deep residual learning for image recognition. In *Proceedings of the IEEE conference on computer vision and pattern recognition*, 770–778.

Jin, M.; Koh, H. Y.; Wen, Q.; Zambon, D.; Alippi, C.; Webb, G. I.; King, I.; and Pan, S. 2023. A Survey on Graph Neural Networks for Time Series: Forecasting, Classification, Imputation, and Anomaly Detection. *arXiv preprint arXiv:2307.03759*.

Kim, T.; Kim, J.; Tae, Y.; Park, C.; Choi, J.-H.; and Choo, J. 2021. Reversible instance normalization for accurate time-series forecasting against distribution shift. In *International Conference on Learning Representations*.

Lai, G.; Chang, W.-C.; Yang, Y.; and Liu, H. 2018. Modeling long-and short-term temporal patterns with deep neural networks. In *The 41st international ACM SIGIR conference on research & development in information retrieval*, 95–104.

Li, F.; Feng, J.; Yan, H.; Jin, G.; Yang, F.; Sun, F.; Jin, D.; and Li, Y. 2023. Dynamic graph convolutional recurrent network for traffic prediction: Benchmark and solution. *ACM Transactions on Knowledge Discovery from Data*, 17(1): 1–21.

Li, Y.; Yu, R.; Shahabi, C.; and Liu, Y. 2018. Diffusion Convolutional Recurrent Neural Network: Data-Driven Traffic Forecasting. In *International Conference on Learning Representations*.

Liu, M.; Zeng, A.; Chen, M.; Xu, Z.; Lai, Q.; Ma, L.; and Xu, Q. 2022. Scinet: Time series modeling and forecasting with sample convolution and interaction. *Advances in Neural Information Processing Systems*, 35: 5816–5828.

Liu, X.; Liang, Y.; Huang, C.; Hu, H.; Cao, Y.; Hooi, B.; and Zimmermann, R. 2023a. Do We Really Need Graph Neural Networks for Traffic Forecasting? *arXiv preprint arXiv:2301.12603*.

Liu, X.; Xia, Y.; Liang, Y.; Hu, J.; Wang, Y.; Bai, L.; Huang, C.; Liu, Z.; Hooi, B.; and Zimmermann, R. 2023b. LargeST: A Benchmark Dataset for Large-Scale Traffic Forecasting. *arXiv preprint arXiv:2306.08259*.

Loukas, A. 2019. What graph neural networks cannot learn: depth vs width. *arXiv preprint arXiv:1907.03199*.

Marisca, I.; Cini, A.; and Alippi, C. 2022. Learning to Reconstruct Missing Data from Spatiotemporal Graphs with Sparse Observations. *arXiv preprint arXiv:2205.13479*.

Nie, T.; Qin, G.; Wang, Y.; and Sun, J. 2023a. Correlating sparse sensing for large-scale traffic speed estimation: A Laplacian-enhanced low-rank tensor kriging approach. *Transportation Research Part C: Emerging Technologies*, 152: 104190.

Nie, T.; Qin, G.; Wang, Y.; and Sun, J. 2023b. Towards better traffic volume estimation: Tackling both underdetermined and non-equilibrium problems via a correlation adaptive graph convolution network. *arXiv preprint arXiv:2303.05660*.

Nie, Y.; Nguyen, N. H.; Sinthong, P.; and Kalagnanam, J. 2022. A Time Series is Worth 64 Words: Long-term Forecasting with Transformers. *arXiv preprint arXiv:2211.14730*.

Oreshkin, B. N.; Amini, A.; Coyle, L.; and Coates, M. 2021. FC-GAGA: Fully connected gated graph architecture for spatio-temporal traffic forecasting. In *Proceedings of the AAAI Conference on Artificial Intelligence*, volume 35, 9233–9241.

Pareja, A.; Domeniconi, G.; Chen, J.; Ma, T.; Suzumura, T.; Kanezashi, H.; Kaler, T.; Schardl, T.; and Leiserson, C. 2020. Evolvegcn: Evolving graph convolutional networks for dynamic graphs. In *Proceedings of the AAAI conference on artificial intelligence*, volume 34, 5363–5370.

Sato, R.; Yamada, M.; and Kashima, H. 2021. Random features strengthen graph neural networks. In *Proceedings of the 2021 SIAM International Conference on Data Mining (SDM)*, 333–341. SIAM.

Satorras, V. G.; Rangapuram, S. S.; and Januschowski, T. 2022. Multivariate Time Series Forecasting with Latent Graph Inference. *arXiv preprint arXiv:2203.03423*.

Sen, R.; Yu, H.-F.; and Dhillon, I. S. 2019. Think globally, act locally: A deep neural network approach to high-dimensional time series forecasting. *Advances in neural information processing systems*, 32.

Shao, Z.; Zhang, Z.; Wang, F.; Wei, W.; and Xu, Y. 2022a. Spatial-Temporal Identity: A Simple yet Effective Baseline for Multivariate Time Series Forecasting. In *Proceedings of the 31st ACM International Conference on Information & Knowledge Management*, 4454–4458.

Shao, Z.; Zhang, Z.; Wei, W.; Wang, F.; Xu, Y.; Cao, X.; and Jensen, C. S. 2022b. Decoupled dynamic spatial-temporal graph neural network for traffic forecasting. *arXiv preprint arXiv:2206.09112*.

Srinivasan, B.; and Ribeiro, B. 2019. On the equivalence between positional node embeddings and structural graph representations. *arXiv preprint arXiv:1910.00452*.

Ulyanov, D.; Vedaldi, A.; and Lempitsky, V. 2016. Instance normalization: The missing ingredient for fast stylization. *arXiv preprint arXiv:1607.08022*.

Vaswani, A.; Shazeer, N.; Parmar, N.; Uszkoreit, J.; Jones, L.; Gomez, A. N.; Kaiser, Ł.; and Polosukhin, I. 2017. Attention is all you need. In *Advances in neural information processing systems*, 5998–6008.

Wu, F.; Souza, A.; Zhang, T.; Fifty, C.; Yu, T.; and Weinberger, K. 2019a. Simplifying graph convolutional networks. In *International conference on machine learning*, 6861–6871. PMLR.

Wu, H.; Hu, T.; Liu, Y.; Zhou, H.; Wang, J.; and Long, M. 2022. TimesNet: Temporal 2D-Variation Modeling for General Time Series Analysis. *arXiv preprint arXiv:2210.02186*.

Wu, Z.; Pan, S.; Long, G.; Jiang, J.; Chang, X.; and Zhang, C. 2020. Connecting the Dots: Multivariate Time Series Forecasting with Graph Neural Networks. In *Proceedings of the 26th ACM SIGKDD International Conference on Knowledge Discovery and Data Mining*, 753–763. New York, NY, USA: Association for Computing Machinery.

Wu, Z.; Pan, S.; Long, G.; Jiang, J.; and Zhang, C. 2019b. Graph Wavenet for Deep Spatial-Temporal Graph Modeling. In *Proceedings of the 28th International Joint Conference on Artificial Intelligence*, 1907–1913.

Xu, M.; Dai, W.; Liu, C.; Gao, X.; Lin, W.; Qi, G.-J.; and Xiong, H. 2020. Spatial-temporal transformer networks for traffic flow forecasting. *arXiv preprint arXiv:2001.02908*.

Yang, C.; Wu, Q.; Wang, J.; and Yan, J. 2022. Graph Neural Networks are Inherently Good Generalizers: Insights by Bridging GNNs and MLPs. *arXiv preprint arXiv:2212.09034*.

Yu, B.; Yin, H.; and Zhu, Z. 2018. Spatio-temporal graph convolutional networks: a deep learning framework for traffic forecasting. In *Proceedings of the 27th International Joint Conference on Artificial Intelligence*, 3634–3640.

Zeng, A.; Chen, M.; Zhang, L.; and Xu, Q. 2022. Are transformers effective for time series forecasting? *arXiv preprint arXiv:2205.13504*.

Zhang, Q.; Chang, J.; Meng, G.; Xiang, S.; and Pan, C. 2020. Spatio-temporal graph structure learning for traffic forecasting. In *Proceedings of the AAAI conference on artificial intelligence*, volume 34, 1177–1185.

Zhang, T.; Zhang, Y.; Cao, W.; Bian, J.; Yi, X.; Zheng, S.; and Li, J. 2022. Less is more: Fast multivariate time series forecasting with light sampling-oriented mlp structures. *arXiv preprint arXiv:2207.01186*.

Zheng, C.; Fan, X.; Wang, C.; and Qi, J. 2020. Gman: A graph multi-attention network for traffic prediction. In *Proceedings of the AAAI Conference on Artificial Intelligence*, volume 34, 1234–1241.